Experimental investigation of the mechanism of supercritical CO$_2$ interaction with tight sandstone

Huan Peng[1,2]*, Jian Yang[1,2], Junliang Peng[1,2], Junhong Pu[3], Qiang Liu[3], Jun Su[1,2] and Jin Liu[4]

[1]Engineering Technology Research Institute of Southwest Oil & Gas Field Company, PetroChina, Chengdu, China, [2]Key Laboratory of Oil & Gas Well Stimulation Technology of Southwest Oil & Gas Field Company, Chengdu, China, [3]Southwest Oil & Gas Field Company, PetroChina, Chengdu, China, [4]No. 8 Oil Extraction Plant of Changqing Oilfield Company, PetroChina, Xi'an, China

One of the important technologies for combating global climate change is CCUS (Carbon Capture, Utilization, and Storage), which aims to address the issue of "greenhouse effect" generated by a significant amount of greenhouse gas emissions. Supercritical CO$_2$, a new type of anhydrous fracturing fluid with broad application prospects in low-pressure tight sandstone gas reservoirs, has several advantages over traditional water-based fracturing fluids, including quick flowback, minimal damage to the reservoir, and the ability to realize *in-situ* storage of greenhouse gases. The tight sandstone cores from the Jinqiu Gas field in the Sichuan Basin were used in an experimental investigation on the interaction mechanism between supercritical CO$_2$ and tight sandstone to examine the viability of supercritical CO$_2$ fracturing with tight sandstone, and analysis of the samples' post-reaction samples' mineral composition, microstructure, mass change, and total salinity change. The interaction of tight sandstone with supercritical CO$_2$ results in an increase in quartz content, a decrease in clay mineral content, the formation of new minerals, and partial mineral dissolution on the surface of the sample. Since the degree of mineral dissolution of sandstone samples increases with time, CO$_2$ can be stored in tight sandstone as carbonate minerals. This study evaluates how supercritical CO$_2$ interacts with tight sandstone and can offer a solid theoretical foundation and experimental evidence in favor of CO$_2$ *in-situ* storage in tight sandstone gas reservoir.

KEYWORDS

supercritical CO$_2$, tight sandstone, interaction mechanism, CCUS, fracturing technology, experimental evaluation

1 Introduction

The "greenhouse effect," which is brought on by a significant quantity of greenhouse gas emissions, has sparked widespread worry as social economy continues to advance and global industrialisation picks up speed. The average CO$_2$ concentration in the atmosphere has risen to its greatest level in almost a million years since the globe started the industrialization era, and temperatures are increasing (Grainger and Smith, 2021). Both

the ecosystem of the world and the advancement of human society are in grave danger. Future climate change will cause a number of chain reactions that will get worse as time goes on, including an increase in extreme weather occurrences, a rise in sea level, and the extinction of marine and terrestrial ecosystems (Zou et al., 2021). If CO_2 emissions continue to climb, the world's temperature will rise by 2°C by the end of the century, the sea level will rise by almost 1 m, most coral reefs will vanish, 13% of terrestrial ecosystems will be lost, and many plants and animals may be in danger (Umar et al., 2022). Although the industrial age has brought about great advancement and ease, it has also led to major environmental issues and unsustainable expansion.

The Paris Climate Agreement, which proposed achieving the goal of "net zero emissions" of CO_2 around 2050, or carbon neutrality, was adopted at the 21st United Nations Climate Change Conference in order to address global climate change (Zhao et al., 2022), realize the advancement of human civilization, and ensure the sustainable development of the earth's ecosystem (Tapia et al., 2018). As a result, countries have adopted policies that reflect the significance of lowering greenhouse gases, particularly CO_2 emissions.

The geological storage method of CO_2 is currently the best efficient way to deal with CO_2, a greenhouse gas. It involves gathering the CO_2 gas produced by fixed point sources (industrial point sources or power plants) and storing it in a reasonably closed geological structure (Hasan et al., 2015). All deep salt water bearing strata, oil and gas reservoirs, barren coal seams, and deep ocean have the perfect storage location. Their individual CO_2 storage mechanisms, however, differ as a result of the various storage sites.
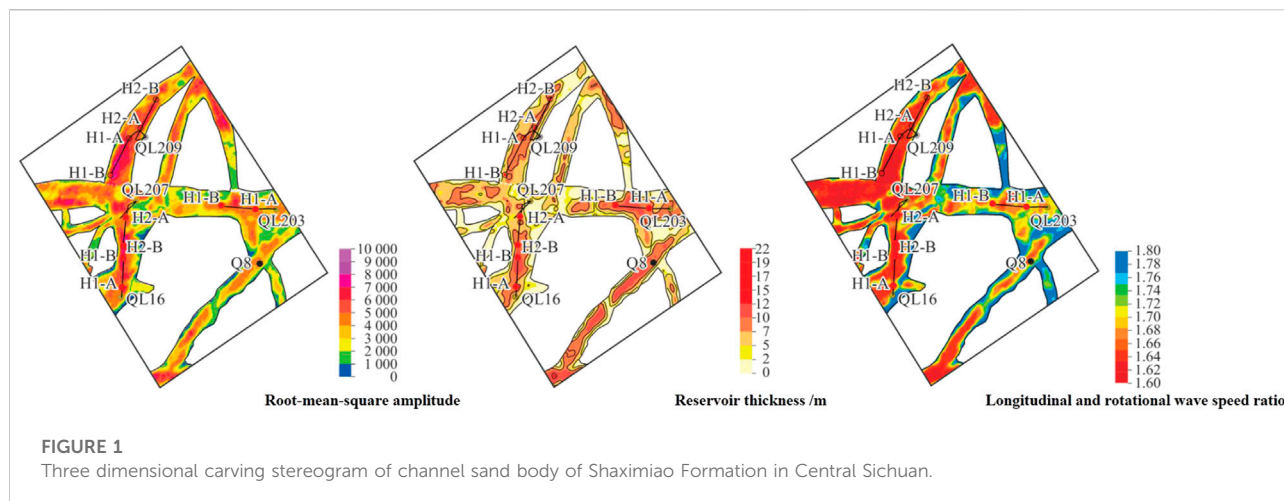
Researchers proposed three pathways for CO_2 disposal in deep saline water layer in the CO_2 storage in deep saline water layer study (Wang et al., 2021). First, in a process known as dissolution landfill technology, CO_2 is directly dissolved in formation water. This approach is expected to raise the acidity of the formation water, which will increase the solubility of minerals in the parent rock because the formation water with CO_2 dissolved is already mildly acidic (Zhou et al., 2019); Second, after CO_2 injection, it directly or indirectly reacts with minerals in the formation to produce secondary carbonate minerals, which are precipitated in the form of new minerals (Zhou et al., 2018). Third, CO_2 is stored under the cover of low permeability rock in the form of gas or supercritical fluid, that is, CO_2 is loaded into "sealed tank," which is typically referred to as liquid landfill technology (Yue et al., 2022). Mineral landfill technique is the name given to this process. This process has a good chance of success since it can solidify CO_2 into a component of solid minerals over an extended period of time.

Theoretical study and practical experience demonstrate that oil and gas reservoirs can store CO_2 for a long period because of their effective capping. The chance of CO_2 stored there leaking out is the smallest compared to other geological entities such deep salt water layers, basalt, and non-minable coal seams.

Additionally, it is easier to store CO_2 and has higher economic benefits now that production wells and injection wells have been constructed in the oil and gas reservoirs. A long-term technique of storing CO_2 is in oil and gas reservoirs. One of the primary methods for storing CO_2 is to inject supercritical CO_2 into oil and gas reservoirs using oil field injection wells or production wells (Bachu, 2016). Therefore, increased oil recovery is paired with CO_2 reservoir storage as the primary method. Oil and gas reservoir storage uses CO_2 to force crude oil to flow to production wells, similar to how water drive enhance oil recovery. The main mechanism of CO_2 oil displacement involves interphase mass transfer, crude oil volume expansion, viscosity reduction, lowering of oil-gas interfacial tension, and oil-gas mixing, all of which occur during the contact between CO_2 and crude oil (Mouahid et al., 2022).

Supercritical CO_2 has been employed as a working fluid in various theoretical and experimental studies in petroleum engineering (Nikolai et al., 2019; Peng et al., 2019), and it can be used to displace oil. Supercritical CO_2 hydraulic fracturing is regarded as one of the most environmentally benign fracturing technologies since it has several benefits in reservoirs (Zhao et al., 2017; Hazarika and Boruah, 2022), particularly for water-sensitive formations (Liu et al., 2014), low pressure reservoirs, and water-stressed regions (Cao et al., 2017). Although it is well known that supercritical CO_2 has many advantages over water-based fracturing fluid, the majority of the work is still done on shale (Jiang et al., 2016; Jia et al., 2018; Memon et al., 2022). For example, the matrix minerals dissolve (Ao et al., 2017), the dissolved minerals precipitate (Chen et al., 2022), the rock breakdown pressure is lowered (Gathitu et al., 2009; Wang et al., 2018; Peng et al., 2020), the rock matrix swells (Day et al., 2008), and so on. Uncertainty exists regarding the exact mechanism of action between supercritical CO_2 and tight sandstone. Tight sandstone and supercritical CO_2 will interact physicochemically during supercritical CO_2 fracturing (Peng et al., 2016). The flow condition of subsurface oil and gas will be impacted by changes in tight sandstone's pore characteristics, porosity, permeability, and other physical qualities (Lin et al., 2008; Lin et al., 2022). The evaluation of the mineral composition, microstructure, mass change, and total salinity change of supercritical CO_2 fracturing in low pressure tight sandstone reservoirs is therefore critical; nevertheless, there have only been a few publications in the literature up to this point.

This study examines the feasibility of fracturing supercritical CO_2 with tight, low-pressure sandstone. We investigate how tight sandstone and supercritical CO_2 interact. Different tight sandstone samples were treated with supercritical CO_2 using the tight sandstone cores from the Jinqiu Gas field in the Sichuan Basin, and the results were evaluated for changes in mineral composition, microstructure, mass change, and total salinity under various time, pressure, and temperature conditions. To

FIGURE 1
Three dimensional carving stereogram of channel sand body of Shaximiao Formation in Central Sichuan.

FIGURE 2
Sampled from tight sandstone cores.

FIGURE 3
Visualization device for rock and supercritical CO_2 interactions.

further enhance the interaction mechanism between supercritical CO_2 and low pressure tight sandstone, quantify the impact of supercritical CO_2 on the mineral composition, microstructure, mass change, and total salinity of tight sandstone. This discovery evaluates the mechanism of supercritical CO_2's interaction with tight sandstone, and it can offer a theoretical foundation and experimental support for CO_2 *in-situ* storage in tight sandstone gas reservoirs.

2 Materials and methods

2.1 Core sample

The channel sand bodies in the Shaximiao Formation in the Sichuan Basin are found to be very developed longitudinally, widely dispersed on the plane, with good reservoir physical properties, and to have great exploration potential, according to recent comprehensive geological research on the Shaximiao

Formation System. The three-dimensional carving stereogram of river sand body is shown in Figure 1 (Zhang and Yang, 2022).

The Shaximiao formation's natural gas has the advantages of shallow burial, low cost, short cycle, and quick effect. At the moment, it is one of the important practical fields of benefit development under low oil prices, and has drawn a lot of attention. Major natural gas exploration breakthroughs have been made in Qiulin, Jinhua, Yanting, and other locations in the central and western Sichuan region. As a result, Shaximiao formation has emerged as the Sichuan Basin's newest focus for oil and gas exploration (Zhang et al., 2022).

The reservoir temperature is 1.9–2.5°C/100 m, the reservoir depth is 1,500–2800 m, the cumulative thickness of the reservoir is 20–70 m, the reservoir porosity is mainly 8%–15%, the permeability is mainly 0.01–1.00 mD, and the pressure coefficient of the seven# sand body is only 0.47, belonging to the normal temperature and low pressure tight sandstone gas reservoir (Zheng et al., 2021).

FIGURE 4
Visualization device for rock and supercritical CO_2 interactions flow chart.
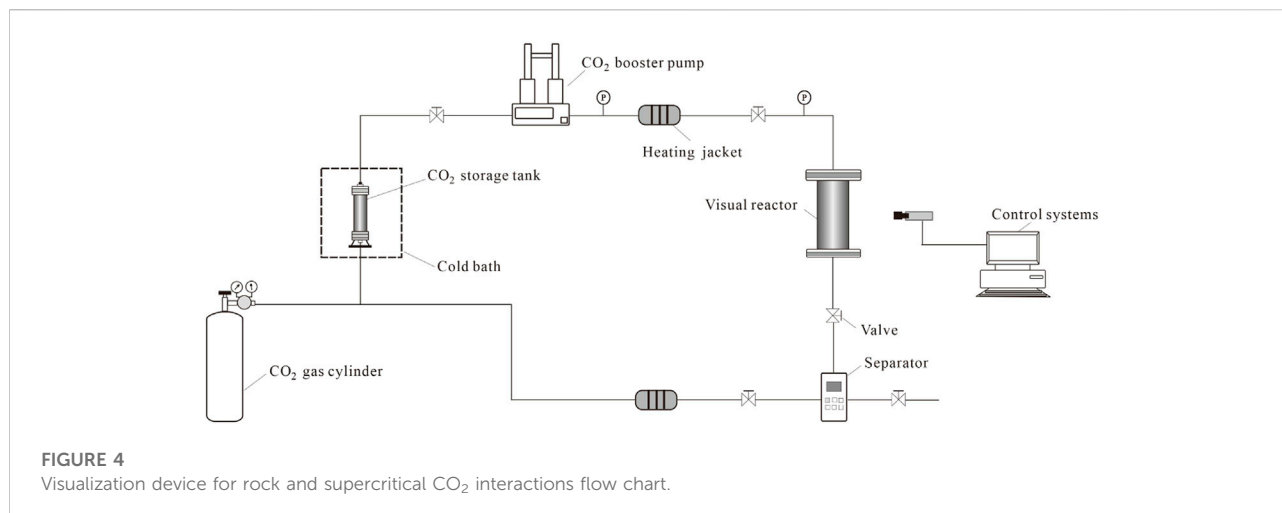
Select a sandstone core that is underground that has a complete exterior and no visible fractures. Drill, cut, and polish the two ends with an end grinder to make sure they are parallel and smooth. The core measures 15 mm in length and 25 mm in diameter, As shown in Figure 2. The end face of the core sample must be vertical to the circumference and the maximum deviation must not be greater than 0.05 mm. The height and diameter errors of the core sample must not be greater than 0.3 mm. The core must be processed in accordance with the standards of the International Society of Rock Mechanics (ISRM) to make the sample error within the following range. The sandstone sample must be wrapped and covered with fresh-keeping film after preparation in order to shield it from air reaction during following studies.

2.2 Apparatus

As shown in Figure 3, the visualization apparatus for the interaction of supercritical CO_2 with rock consists of a CO_2 gas cylinder, a CO_2 storage tank, a cold bath, a CO_2 booster pump, a visual reactor, a heating jacket, and control systems. Visual reactor is a crucial part of the experimental system. As seen in Figure 3, the sapphire glass window in the visual reactor allows for real-time observation of the interaction process between supercritical CO_2 and rock. The visual reactor has a volume of 500 ml, the CO_2 storage tank has a volume of 5 L, the temperature range is $-5°C–150°C$, and the pressure bearing capability of the entire unit is 50 MPa. The flow chart of the experimental device is shown in Figure 4. By using the control system and changing the settings of the heating jacket and CO_2 booster pump, the liquid CO_2 is converted to supercritical CO_2, as shown in Figure 5, which can be used for the interaction process between supercritical CO_2 and rock at different temperatures, pressures and times.

The scanning electron microscopy apparatus is represented in Figure 6, and it is primarily made up of an electron

FIGURE 5
CO_2 phase diagram.
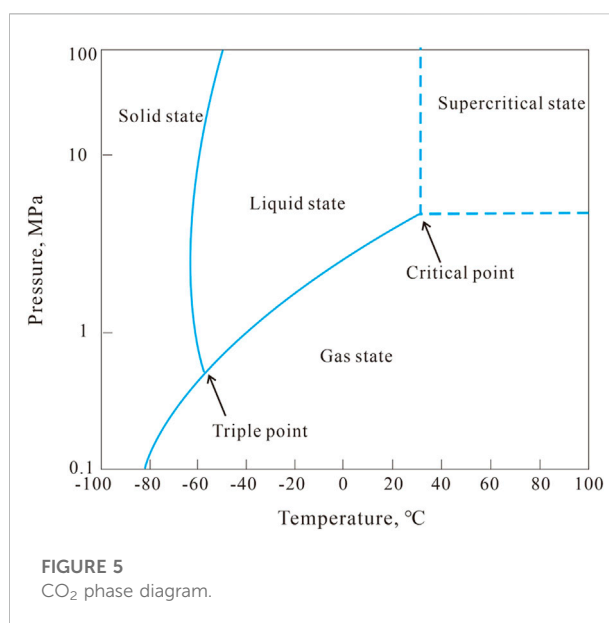
microscope, an electron gun filament, a vacuum system, and an automated system for acquiring and processing samples and images. With a maximum magnification of ×150000 and a resolution higher than 10 nm, it can swiftly produce images with rich surface features that can be used to measure samples that are smaller than a micron or even smaller than a nanometer in size. It is used to research how supercritical CO_2 interacts with rock and to track trends in reservoir physical qualities like permeability and porosity.

Figure 7 shows an X-ray diffractometer. A high stability X-ray source, a sample and sample position orientation adjustment mechanism system, a ray detector, and a system for processing and analyzing diffraction patterns make up its core parts. Equipment specifications: A common size light tube is used

FIGURE 6
Scanning electron microscopes equipment.

FIGURE 7
X-ray diffractometer.

FIGURE 8
Ion chromatograph.

as the Cu target, and a theta/theta vertical goniometer is used. The theta angle range is 2–160, and the angle accuracy is 0.0001. The X-ray needed for measurement is produced by the high stability X-ray source. The X-ray tube's anode target material

can alter the wavelength of the radiation. The intensity of the X-ray source can be changed by adjusting the anode voltage. This allows for routine phase analysis and semi-quantitative analysis of polycrystalline powder, block, and liquid samples, as well as the determination and correction of unit cell parameters, the X-ray diffraction indexation of unidentified polycrystalline samples, and the determination of grain size and crystallinity.

The flow compatibilizer, high-pressure infusion pump, sampler, chromatographic column, detector, and data processing system are the key components of the ion chromatograph, as shown in Figure 8. The chromatographic pump has a maximum operating pressure of 50 MPa, a flow rate of 0.001–20 ml/min, a minimum graduation value of 0.001 ml/min, a concentration range of 0–100% for the ion chromatograph's eluent, an effective injection volume of 0.5–11 ml, and a measurement range of 0–15000 us/cm without section switching. The plasma concentrations of K^+, Na^+, Ca^{2+}, Mg^{2+}, Cl^-, F^-, and SO_4^{2-} in aqueous solution are used in a liquid chromatography method for separation and detection that uses the ionic properties of the tested substances. This method is a powerful reference for the variation characteristics and laws of ion concentration in liquid.

2.3 Methods

It is required to examine and identify changes in the microscopic properties, mineral composition, and ion concentration of the solution of sandstone samples before and after the experiment in order to research the mechanism of interaction between supercritical CO_2 and sandstone. The steps of the experiment are as follows:

1) In order to accurately obtain the change of core weight, sandstone samples should be cleaned with distilled water to remove surface impurities, and then dried and weighed.
2) Assemble the visualization tool for the interaction between supercritical CO_2 and rock and wait until it is ready for usage. It is used to carry out the interaction process between supercritical CO_2 and tight sandstone.
3) Place the formation water-prepared container into the visualization device for the interaction between supercritical CO_2 and rock, then insert it into the sandstone core. Next, start the booster pump to inject CO_2 for pressurization. Then, set the pressurization temperature and time according to different experiments. Finally, determine the sampling times according to the time. Take a core and 20 ml of liquid each time, and inspect and analyze the core with scanning electron microscopy.
4) After the reaction, allow the reactor to cool to ambient temperature before opening it to remove the sample. The sandstone sample should then be cleaned with distilled water, dried, and weighed in an oven.

TABLE 1 Tight sandstone weight variation after supercritical CO_2 at various times.

Project	Test time, h		
	48	168	360
Tight sandstone weight before being treated to supercritical CO_2, g	17.6625	17.6319	17.6132
Tight sandstone weight after being treated to supercritical CO_2, g	17.3251	17.1239	16.7597
Weight change of tight sandstone, g	0.3374	0.5080	0.8535
Tight sandstone's rate of weight change, %	1.91	2.88	4.85

5) Following the aforementioned treatment, the core was examined and evaluated using a scanning electron microscope and an X-ray diffractometer; an ion chromatograph was used to ascertain the composition of the reaction solution. The interaction mechanism between supercritical CO_2 and tight sandstone is analyzed.

3 Process of supercritical CO_2 reacting with tight sandstone

When supercritical CO_2 comes into contact with sandstone at the proper temperature and pressure, it first diffuses into the rock aquifer's pores, interacts with formation water to form a weak acidic fluid, and then reacts with the rocks to produce a series of complicated chemical reactions that lead to the decomposition of brittle minerals like carbonate and feldspar in the sandstone and the precipitation of new minerals, altering the microstructure, weight, porosity, and permeability of sandstone.
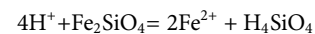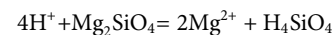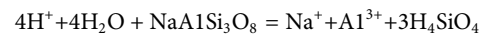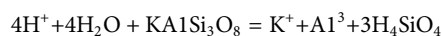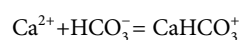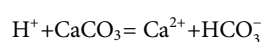
The fluid changes into a weak acidic fluid as a result of CO_2 first coming into touch with the water in the pores, followed by it dissolving in the water at the water-air interface and reacting with it to generate carbonic acid (Bierg and Banwart, 2000). The reaction formula is:
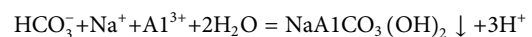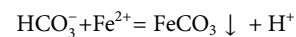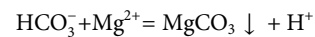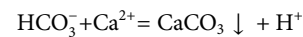
$$CO_2 + H_2O = H_2CO_3$$
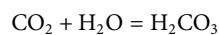
Carbonic acid quickly breaks down into bicarbonate ions:

$$H_2CO_3 = H^+ + HCO_3^-$$
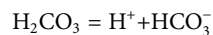
The released hydrogen ions will result in the complexation of dissolved cations with bicarbonate ions and the disintegration of carbonate minerals and silicates in tight sandstone rocks, including:

$$H^+ + CaCO_3 = Ca^{2+} + HCO_3^-$$
$$Ca^{2+} + HCO_3^- = CaHCO_3^+$$
$$4H^+ + 4H_2O + KA1Si_3O_8 = K^+ + A1^{3+} + 3H_4SiO_4$$

$$4H^+ + 4H_2O + NaA1Si_3O_8 = Na^+ + A1^{3+} + 3H_4SiO_4$$
$$4H^+ + Mg_2SiO_4 = 2Mg^{2+} + H_4SiO_4$$
$$4H^+ + Fe_2SiO_4 = 2Fe^{2+} + H_4SiO_4$$

Finally, the dissolved bicarbonate combines with cations to produce additional carbonate minerals such as calcite, magnesite, siderite, and dawsonite:

$$HCO_3^- + Ca^{2+} = CaCO_3 \downarrow + H^+$$
$$HCO_3^- + Mg^{2+} = MgCO_3 \downarrow + H^+$$
$$HCO_3^- + Fe^{2+} = FeCO_3 \downarrow + H^+$$
$$HCO_3^- + Na^+ + A1^{3+} + 2H_2O = NaA1CO_3(OH)_2 \downarrow + 3H^+$$

Therefore, soluble minerals in the rock are dissolved after CO_2 and tight sandstone come into contact, and new minerals are also generated, modifying the sandstone.

4 Results and discussion

4.1 Effect of supercritical CO_2 on the weight of tight sandstone

According to the formation conditions and the characteristic time stage after simulated fracturing treatment. Tight sandstone and supercritical CO_2 reaction for 48, 168, and 360 h, respectively, at 60°C under a test pressure of 10 MPa, the temperature is the formation temperature, the pressure is the difference between the minimum principal stress of the formation and the formation pore pressure, and the action time is selected as several characteristic time points after fracturing treatment. The samples of sandstone are weighed after the reaction. Table 1 shows the test results. The weight of the rocks decreases after the test. After supercritical CO_2 dissolves in water, the hydrogen ions decomposed by weak acidic fluid dissolve potassium feldspar, plagioclase and some clay minerals, resulting in rock weight changes. The weight of the tight sandstone samples reduces by 1.91% after 48 h, 2.88% after 168 h, and 4.85% after 360 h. More weight loss over time suggests that the supercritical CO_2 and rock primarily have a certain
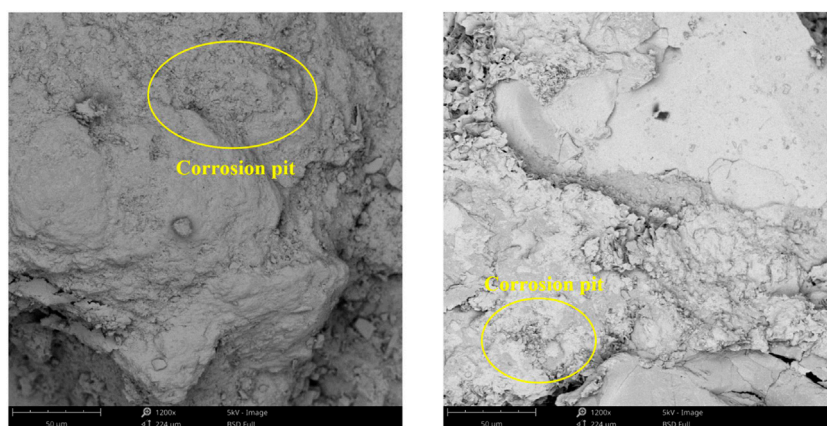
FIGURE 9
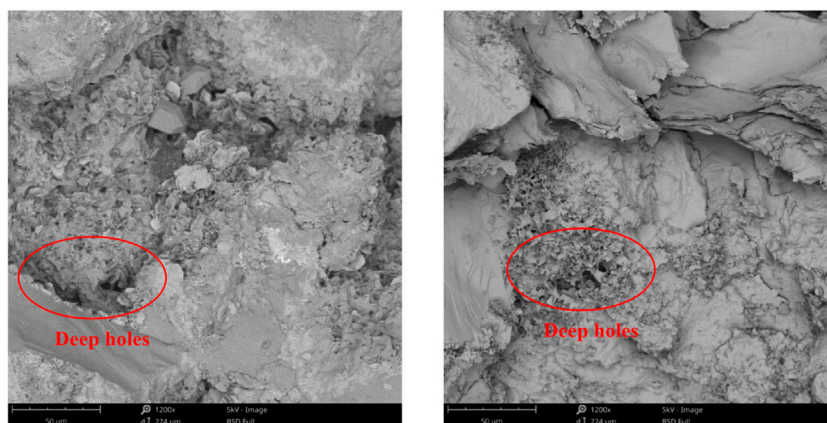Effect of supercritical CO$_2$ on microstructure of tight sandstone (After 48 h).

FIGURE 10
Effect of supercritical CO$_2$ on microstructure of tight sandstone (After 168 h).

dissolving response during the experiment, and that the degree of dissolution gradually increases as time goes on.

4.2 Effect of supercritical CO$_2$ on microstructure of tight sandstone

Tight sandstone and supercritical CO$_2$ reacted at 60°C for 48 h, 168 h, and 360 h, respectively, under an experimental pressure of 10 MPa. After the reaction, sandstone samples were examined under a scanning electron microscope to reveal that after 48 h, the feldspar was only mildly corroded while the quartz and clay minerals remained comparatively stable, generating a few corrosion pits, as seen in Figure 9. As depicted in Figure 10, after 168 h of reaction, the degree of feldspar dissolution increased, quartz and clay minerals also started to undergo weak dissolution, and some deep holes developed on the visible surface; After 360 h of reaction, the feldspar's degree of dissolution increased further, and quartz and clay minerals started to dissolve somewhat as well, resulting in a broken dissolution phenomena, as illustrated in Figure 11.

4.3 Effect of supercritical CO$_2$ on mineral composition of tight sandstone

When CO$_2$ is in a supercritical state, it reacts with tight sandstone. It initially diffuses into the tight sandstone aquifer pores at formation temperature and pressure, reacts with formation water to form weak acidic fluid, and then interacts with rocks to produce a series of intricate chemical processes.

TABLE 2 Initial sample samples' mineral composition.

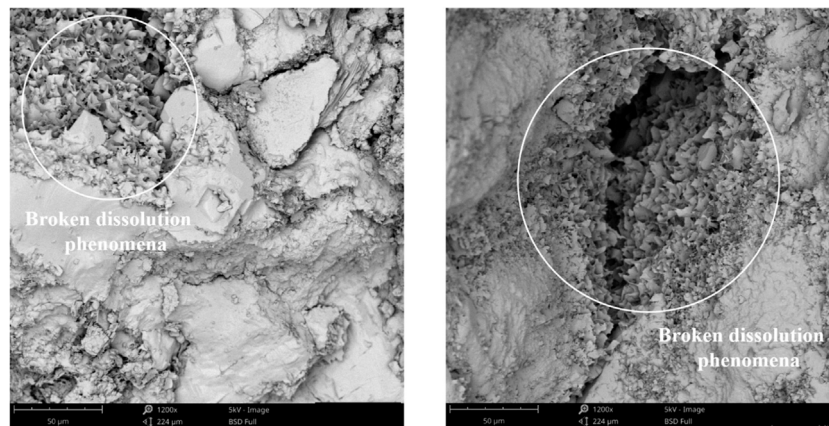| Component type	Quartz	Potassium feldspar	Plagioclase	Clay
Content, %	54.2	2.8	34.5	8.5

FIGURE 11
Effect of supercritical CO_2 on microstructure of tight sandstone (After 360 h).
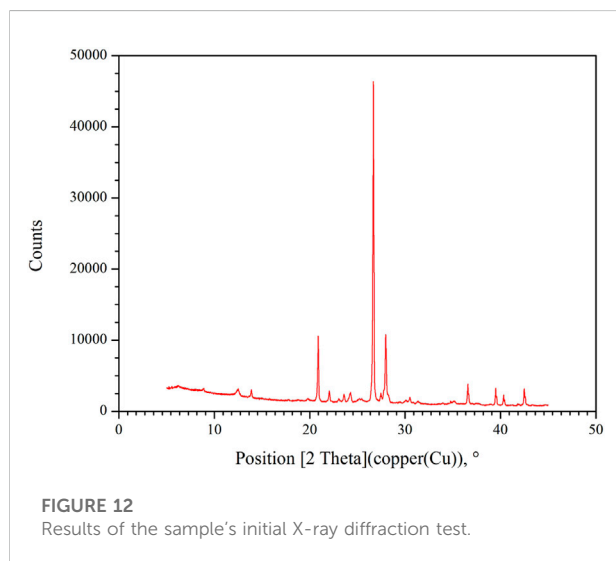

FIGURE 12
Results of the sample's initial X-ray diffraction test.

The mineral compositions of sandstone before and after supercritical CO_2 and tight sandstone were qualitatively and quantitatively examined by XRD in order to further characterize the CO_2 water rock interaction mechanism.

In Figure 12 and Table 2, the results of the analysis and interpretation of the relative content test of mineral components of tight sandstone samples prior to the action of supercritical CO_2 are displayed. The examination of sandstone composition shows that Jinqiu tight sandstone has the highest concentrations of quartz and plagioclase, at 54.2% and 34.5%, respectively.

The tight sandstone reacts with supercritical CO_2 after 48 h, 168 h, and 360 h at 60°C under an experimental pressure of 10 MPa. The sandstone samples are analyzed by X-ray diffraction after the reaction. In Figure 13, the experimental results are displayed.

Following the experiment, the sandstone's material composition was compared and examined. It can be seen that after 48 h of reaction with supercritical CO_2, the quartz content of Jinqiu tight sandstone increased by 1.5%, the potassium feldspar content decreased by 0.2%, the plagioclase content decreased by 1.2%, and the clay minerals content decreased by 0.4%. 0.3% of newly formed calcite was discovered at the same time. After 168 h of reaction, quartz's content increased by 3.4%, potassium feldspar's content dropped by 0.7%, plagioclase's content dropped by 2.8%, the content of clay minerals dropped by 0.6%, and the content of newly formed calcite increased to 0.7%. After 360 h of reaction, there was a 5.3% increase in quartz content, a 1.1% decrease in potassium feldspar content, a 4.3% drop in plagioclase content, a 1.0% decrease in clay mineral content, and a 1.0% increase in newly created calcite content.

Generally speaking, when supercritical CO_2 interacts with Jinqiu tight sandstone, quartz content rises, potassium feldspar

FIGURE 13
Mineral composition of tight sandstone changes after various supercritical CO_2 reaction times.
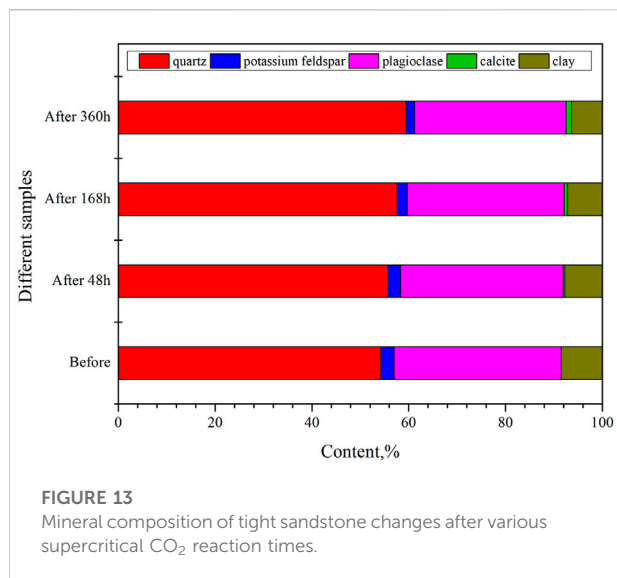
and plagioclase content fall, and new calcite minerals form. Thus, it is clear how the ionic reaction $Ca^{2+} + CO_3^{2-} \leftrightarrows CaCO_3$ (calcite) in the solution and the deposition of the resulting calcite on the sample surface occur during the experiment as a result of the interaction between CO_2 and the sandstone samples. It is possible to implement the underground storage of CO_2 using material traps, as evidenced by the development of calcite, which shows that CO_2 can be stored in the solution as insoluble carbonate and precipitated as calcite and other CO_2 capture minerals.

4.4 Effect of supercritical CO_2 on solution composition

Feldspar, quartz, and other soluble minerals in the reservoir sandstone can dissolve in the acidic fluid created when CO_2 dissolves in water, creating new carbonate minerals. The formation temperature and pressure of the reservoir are simulated in accordance with the detection results of the formation water quality of the reservoir in order to further study the dissolution of feldspar, quartz, clay minerals, and other soluble minerals, combined with the change of ion

concentration in the reaction solution. The production of CO_2 fluid and the interaction of water and sandstone are further discussed.

After completely soaking the dense sandstone samples, Table 3 displays the formation water data of the sha1-2 sub member of the Shaximiao Formation in the Jinqiu gas field. $CaCl_2$ type formation water is used. According to the salt formed by the final combination of Na^+, Cl^- and other ions, the name of this kind of salt is water type. It mainly includes $NaHCO_3$ type, Na_2SO_4 type, $MgCl_2$ type and $CaCl_2$ type. $CaCl_2$ type formation water represents the water formed under the deep closed structural environment, with good sealing property, which is conducive to the accumulation and preservation of oil and gas, and is a sign of good oil and gas.

The tight sandstone reacts with supercritical CO_2 over 48 h, 168 h, and 360 h at 60°C under a test pressure of 10 MPa. Following the reaction, the water quality of the solution containing the samples of sandstone is examined and evaluated. Figure 14 displays the examination results.

In cations, the mass concentrations of K^+, Na^+, Ca^{2+} increased with reaction time. K^+ mainly came from the dissolution of potassium feldspar, and the K^+ concentration increased from 5,133 mg/L to 5,339 mg/L, an increase of 206 mg/L. Na^+ and Ca^{2+} are mainly from the dissolution of plagioclase, indicating that the dissolution degree of potassium feldspar and plagioclase is gradually increasing. The concentration of Na^+ increases from 6,227 mg/L to 6,401 mg/L, an increase of 174 mg/L, and the concentration of Ca^{2+} increases from 18,000 mg/L to 18,200 mg/L, an increase of 200 mg/L. The mass concentration of Mg^{2+} and Ba^{2+} changed slightly with time. The concentration of Mg^{2+} increased from 233 mg/L to 272 mg/L, increased by 39 mg/L, the concentration of Ba^{2+} increased from 1815 mg/L to 1821 mg/L, increased by 6 mg/L, and Al^{3+} also increased from nothing, but the content was low. Al^{3+} concentration increased from 0 mg/L to 12 mg/L, an increase of 12 mg/L.

In anions, a small amount of clay minerals dissolved, resulting in a slow increase in anionic Cl^- concentration, which increased from 51,323 mg/L to 51,569 mg/L, an increase of 246 mg/L. The mass concentration of SO_4^{2-} changed little, and the concentration of SO_4^{2-} increased from 5 mg/L to 12 mg/L, an increase of 7 mg/L. The concentrations of HCO_3^- and CO_3^{2-} in the solution first increased rapidly, and then the growth rate gradually decreased. HCO_3^-

TABLE 3 Initial ion content of formation water.

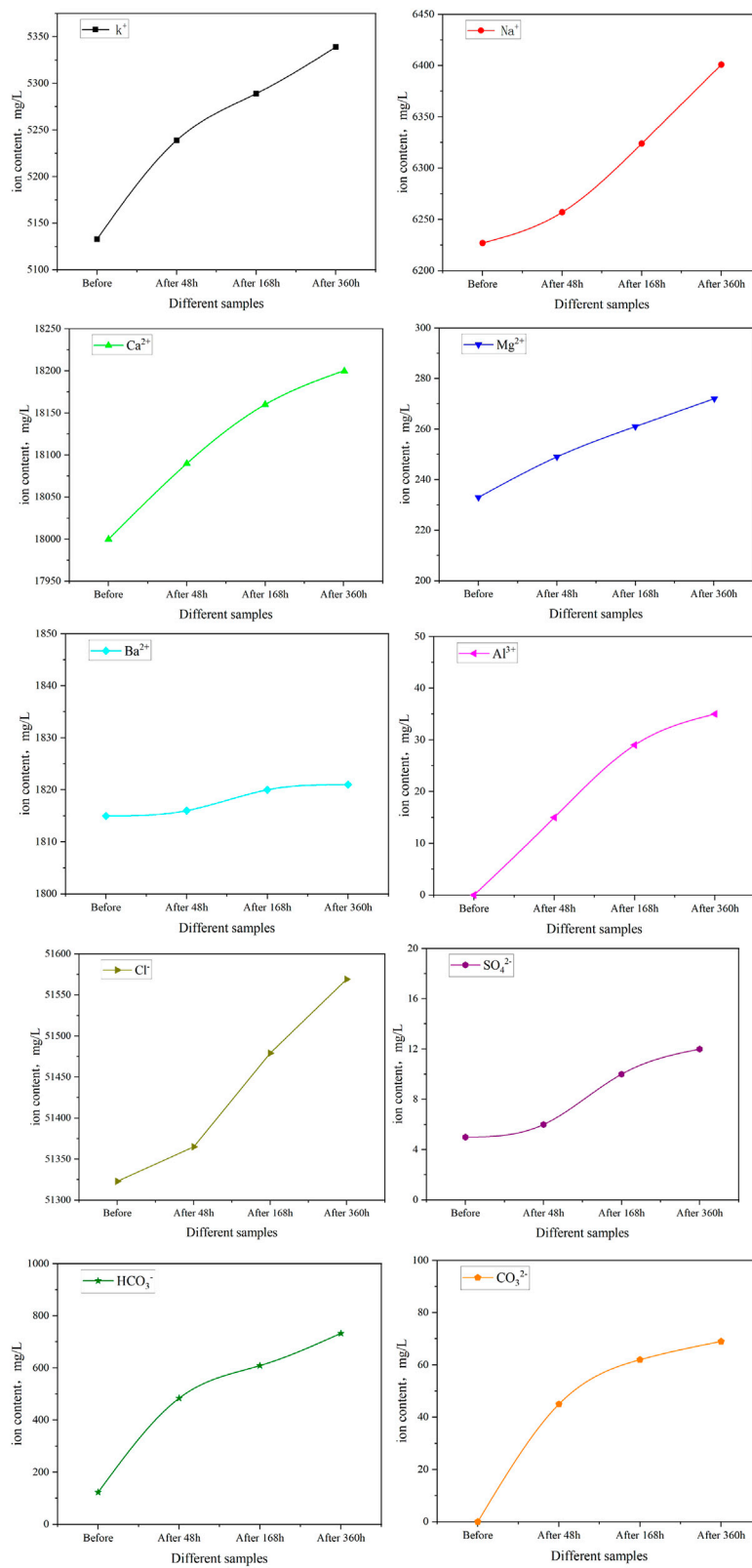| Water type	Ion content of formation water, mg/L							
	Cation					**Anion**		
	K^+	$Na+$	Ca^{2+}	Mg^{2+}	Ba^{2+}	Cl^-	$SO4^{2-}$	$HCO3^-$
$CaCl_2$	5,133	6,227	18,000	233	1815	51,323	5	123

FIGURE 14
Change of mineral composition of after different action time of sandstone and supercritical CO_2.

concentration increased from 123 mg/L to 733 mg/L, an increase of 610 mg/L. The concentration of CO_3^{2-} increased from 0 mg/L to 69 mg/L, an increase of 69 mg/L. The two reactions $H_2CO_3 = H^+ + HCO_3^-$ and $HCO_3^- = H^+ + CO_3^{2-}$ can be used to illustrate the changing process. The CO_3^{2-} is consumed by the reaction equation ($HCO_3^- = H^+ + CO_3^{2-}$), which causes the divalent cations dispersed in the solution and CO_3^{2-} to form insoluble carbonate. As the minerals dissolve, the divalent cations dissolve and produce carbonate precipitation, which slows the pace at which HCO_3^- and CO_3^{2-} concentrations develop in the solution.

5 Summary and conclusions

1) Supercritical CO_2 is a new type of anhydrous fracturing fluid that can achieve *in-situ* storage of greenhouse gases and has a wide range of potential applications in low-pressure tight sandstone gas reservoirs. It differs from conventional water-based fracturing fluid in that it can achieve *in-situ* storage of greenhouse gases.

2) In this study, tight sandstone reacts with supercritical CO_2 after 360 h at 60°C under pressure of 10 MPa, there was a 5.3% increase in quartz content, a 1.1% decrease in potassium feldspar content, a 4.3% drop in plagioclase content, a 1.0% decrease in clay mineral content, and a 1.0% increase in newly created calcite content. Time increases the degree to which sandstone samples dissolve, and CO_2 can be tightly trapped in sandstone as carbonate minerals.

3) After the tight sandstone reacts with supercritical CO_2. In cations, the mass concentrations of K^+, Na^+, Ca^{2+} increased with reaction time, indicating that the dissolution degree of potassium feldspar and plagioclase is gradually increasing. The mass concentration of Mg^{2+} and Ba^{2+} changed slightly with time. In anions, a small amount of clay minerals dissolved, resulting in a slow increase in anionic Cl^- concentration. The mass concentration of SO_4^{2-} changed little. The concentrations of HCO_3^- and CO_3^{2-} in the solution first increased rapidly, and then the growth rate gradually decreased.The interaction mechanism between supercritical CO_2 and sandstone is very important for understanding the feasibility, long-term and safety of CO_2 underground storage and supercritical CO_2 fracturing.

Data availability statement

The original contributions presented in the study are included in the article/Supplementary Material, further inquiries can be directed to the corresponding author.

Author contributions

HP is responsible for the overall structure and revision. JY, JLP, JHP, and QL help evaluate and improve the paper. JS and JL help in setting up the device test, writing, and the experiment.

Funding

Conflict of interest

Authors HP, JY, JLP and JS were employed by Engineering Technology Research Institute of Southwest Oil & Gas Field Company, PetroChina and Key Laboratory of Oil & Gas Well Stimulation Technology of Southwest Oil & Gas Field Company JHP and QL were employed by Southwest Oil & Gas Field Company, PetroChina. JL was employed by No. 8 Oil Extraction Plant of Changqing Oilfield Company, PetroChina.

Publisher's note

All claims expressed in this article are solely those of the authors and do not necessarily represent those of their affiliated organizations, or those of the publisher, the editors and the reviewers. Any product that may be evaluated in this article, or claim that may be made by its manufacturer, is not guaranteed or endorsed by the publisher.

References

Ao, X., Lu, Y., Tang, J., Chen, Y., and Li, H. (2017). Investigation on the physics structure and chemical properties of the shale treated by supercritical CO_2. *J. CO_2 Util.* 20, 274–281. doi:10.1016/j.jcou.2017.05.028

Bachu, S. (2016). Identification of oil reservoirs suitable for CO_2-EOR and CO_2 storage (CCUS) using reserves databases, with application to Alberta, Canada. *Int. J. Greenh. Gas Control* 44, 152–165. doi:10.1016/j.ijggc.2015.11.013

Berg, A., and Banwart, S. A. (2000). Carbon dioxide mediated dissolution of Ca-feldspar: Implications for silicate weathering. *Chem. Geol.* 163 (1-4), 25–42. doi:10.1016/s0009-2541(99)00132-1

Cao, Y., Zhang, J., Zhai, H., Fu, G., Tian, L., and Liu, S. (2017). CO_2 gas fracturing: A novel reservoir stimulation technology in low permeability gassy coal seams. *Fuel* 203, 197–207. doi:10.1016/j.fuel.2017.04.053

Chen, K., Liu, X., Nie, B., Zhang, C., Song, D., Wang, L., et al. (2022). Mineral dissolution and pore alteration of coal induced by interactions with supercritical CO_2. *Energy* 248, 123627. doi:10.1016/j.energy.2022.123627

Day, S., Fry, R., and Sakurovs, R. (2008). Swelling of Australian coals in supercritical CO_2. *Int. J. Coal Geol.* 74 (1), 41–52. doi:10.1016/j.coal.2007.09.006

Gathitu, B. B., Chen, W. Y., and McClure, M. (2009). Effects of coal interaction with supercritical CO_2: Physical structure. *Ind. Eng. Chem. Res.* 48 (10), 5024–5034. doi:10.1021/ie9000162

Grainger, A., and Smith, G. (2021). The role of low carbon and high carbon materials in carbon neutrality science and carbon economics. *Curr. Opin. Environ. Sustain.* 49, 164–189. doi:10.1016/j.cosust.2021.06.006

Hasan, M. F., First, E. L., Boukouvala, F., and Floudas, C. A. (2015). A multi-scale framework for CO_2 capture, utilization, and sequestration: CCUS and CCU. *Comput. Chem. Eng.* 81, 2–21. doi:10.1016/j.compchemeng.2015.04.034

Hazarika, S., and Boruah, A. (2022). Supercritical CO_2 (SCO_2) as alternative to water for shale reservoir fracturing. *Mater. Today Proc.* 50, 1754–1757. doi:10.1016/j.matpr.2021.09.187

Jia, Y., Lu, Y., Elsworth, D., Fang, Y., and Tang, J. (2018). Surface characteristics and permeability enhancement of shale fractures due to water and supercritical carbon dioxide fracturing. *J. Petroleum Sci. Eng.* 165, 284–297. doi:10.1016/j.petrol.2018.02.018

Jiang, Y., Luo, Y., Lu, Y., Qin, C., and Liu, H. (2016). Effects of supercritical CO_2 treatment time, pressure, and temperature on microstructure of shale. *Energy* 97, 173–181. doi:10.1016/j.energy.2015.12.124

Lin, H., Fujii, T., Takisawa, R., Takahashi, T., and Hashida, T. (2008). Experimental evaluation of interactions in supercritical CO_2/water/rock minerals system under geologic CO_2 sequestration conditions. *J. Mat. Sci.* 43 (7), 2307–2315. doi:10.1007/s10853-007-2029-4

Lin, R., Yu, Z., Zhao, J., Dai, C., Sun, Y., Ren, L., et al. (2022). Experimental evaluation of tight sandstones reservoir flow characteristics under CO_2–brine–rock multiphase interactions: A case study in the chang 6 layer, ordos basin, China. *Fuel* 309, 122167. doi:10.1016/j.fuel.2021.122167

Liu, H., Wang, F., Zhang, J., Meng, S., and Duan, Y. (2014). Fracturing with carbon dioxide: Application status and development trend. *Petroleum Explor. Dev.* 41 (4), 513–519. doi:10.1016/s1876-3804(14)60060-4

Memon, S., Feng, R., Ali, M., Bhatti, M. A., Giwelli, A., Keshavarz, A., et al. (2022). Supercritical CO_2-Shale interaction induced natural fracture closure: Implications for scCO2 hydraulic fracturing in shales. *Fuel* 313, 122682. doi:10.1016/j.fuel.2021.122682

Mouahid, A., Claeys-Bruno, M., Bombarda, I., Amat, S., Ciavarella, A., Myotte, E., et al. (2022). Supercritical CO_2 extraction of oil from Moroccan unroasted Argan Kernels: Effects of process parameters to produce cosmetic oil. *J. CO_2 Util.* 59, 101952. doi:10.1016/j.jcou.2022.101952

Nikolai, P., Rabiyat, B., Aslan, A., and Ilmutdin, A. (2019). Supercritical CO_2: Properties and technological applications-A review. *J. Therm. Sci.* 28 (3), 394–430. doi:10.1007/s11630-019-1118-4

Peng, Y., Li, Y., and Zhao, J. (2016). A novel approach to simulate the stress and displacement fields induced by hydraulic fractures under arbitrarily distributed inner pressure. *J. Nat. Gas Sci. Eng.* 35, 1079–1087. doi:10.1016/j.jngse.2016.09.054

Peng, Y., Zhao, J., Sepehrnoori, K., Li, Y., and Li, Z. (2020). The influences of stress level, temperature, and water content on the fitted fractional orders of geomaterials. *Mech. Time. Depend. Mat.* 24 (2), 221–232. doi:10.1007/s11043-019-09417-0

Peng, Y., Zhao, J., Sepehrnoori, K., Li, Z., and Xu, F. (2019). Study of delayed creep fracture initiation and propagation based on semi-analytical fractional model. *Appl. Math. Model.* 72, 700–715. doi:10.1016/j.apm.2019.03.034

Tapia, J. F. D., Lee, J. Y., Ooi, R. E., Foo, D. C., and Tan, R. R. (2018). A review of optimization and decision-making models for the planning of CO_2 capture, utilization and storage (CCUS) systems. *Sustain. Prod. Consum.* 13, 1–15. doi:10.1016/j.spc.2017.10.001

Umar, M., Farid, S., and Naeem, M. A. (2022). Time-frequency connectedness among clean-energy stocks and fossil fuel markets: Comparison between financial, oil and pandemic crisis. *Energy* 240, 122702. doi:10.1016/j.energy.2021.122702

Wang, J., Elsworth, D., Wu, Y., Liu, J., Zhu, W., and Liu, Y. (2018). The influence of fracturing fluids on fracturing processes: A comparison between water, oil and SC-CO_2. *Rock Mech. Rock Eng.* 51 (1), 299–313. doi:10.1007/s00603-017-1326-8

Wang, N., Akimoto, K., and Nemet, G. F. (2021). What went wrong? Learning from three decades of carbon capture, utilization and sequestration (CCUS) pilot and demonstration projects. *Energy Policy* 158, 112546. doi:10.1016/j.enpol.2021.112546

Yue, P., Zhang, R., Sheng, J. J., Yu, G., and Liu, F. (2022). Study on the influential factors of CO_2 storage in low permeability reservoir. *Energies* 15 (1), 344. doi:10.3390/en15010344

Zhang, B. J., Pan, K., and Wu, C. J. (2022). Compound gas accumulation mechanism and model of jurassic Shaximiao formation multistage sandstone formations in Jinqiu field of the Sichuan Basin. *Nat. Gas. Ind.* 42 (1), 51–61. doi:10.3787/j.issn.1000-0976.2022.01.005

Zhang, D. W., and Yang, Y. (2022). Exploration potential and development direction of continental tight sandstone gas in the Sichuan Basin[J]. *Nat. Gas. Ind.* 42 (1), 1–11. doi:10.3787/j.issn.1000-0976.2022.01.001

Zhao, J., Peng, Y., Li, Y., and Tian, Z. (2017). Applicable conditions and analytical corrections of plane strain assumption in the simulation of hydraulic fracturing. *Petroleum Explor. Dev.* 44 (3), 454–461. doi:10.1016/s1876-3804(17)30052-6

Zhao, X., Ma, X., Chen, B., Shang, Y., and Song, M. (2022). Challenges toward carbon neutrality in China: Strategies and countermeasures. *Resour. Conservation Recycl.* 176, 105959. doi:10.1016/j.resconrec.2021.105959

Zheng, Y., Han, X., Zeng, J., Zhou, C., Zhou, L., and Chen, W. (2021). Practice of high-intensity volume fracturing in the Shaximiao Formation tight sandstone gas reservoirs of the Qiulin Block, central Sichuan Basin. *Nat. Gas. Ind. B* 8 (4), 367–375. doi:10.1016/j.ngib.2021.07.007

Zhou, D., Zhang, G., Prasad, M., and Wang, P. (2019). The effects of temperature on supercritical CO_2 induced fracture: An experimental study. *Fuel* 247, 126–134. doi:10.1016/j.fuel.2019.02.099

Zhou, J., Xie, S., Jiang, Y., Xian, X., Liu, Q., Lu, Z., et al. (2018). Influence of supercritical CO_2 exposure on CH_4 and CO_2 adsorption behaviors of shale: Implications for CO_2 sequestration. *Energy fuels.* 32 (5), 6073–6089. doi:10.1021/acs.energyfuels.8b00551

Zou, C., Xue, H., Xiong, B., Zhang, G., Pan, S., Jia, C., et al. (2021). Connotation, innovation and vision of "carbon neutrality". *Nat. Gas. Ind. B* 8 (5), 523–537. doi:10.1016/j.ngib.2021.08.009